Available online at www.sciencedirect.com
ScienceDirect
Journal of Structural Biology 159 (2007) 206–221
Journal of Structural Biology
www.elsevier.com/locate/yjsbi

In vitro selection and characterization of DARPins and Fab fragments for the co-crystallization of membrane proteins: The Na^+-citrate symporter CitS as an example

Thomas Huber, Daniel Steiner, Daniela Röthlisberger [1], Andreas Plückthun *

Department of Biochemistry, University of Zürich, Winterthurerstrasse 190, CH-8057 Zürich, Switzerland

Received 1 December 2006; accepted 26 January 2007
Available online 3 February 2007

Abstract

The determination of 3D structures of membrane proteins is still extremely difficult. The co-crystallization with specific binding proteins may be an important aid in this process, as these proteins provide rigid, hydrophilic surfaces for stable protein–protein contacts. Also, the conformational homogeneity of the membrane protein may be increased to obtain crystals suitable for high resolution structures. Here, we describe the efficient generation and characterization of Designed Ankyrin Repeat Proteins (DARPins) as specific binding molecules for membrane proteins. We used both phage display and ribosome display to select DARPins *in vitro* that are specific for the detergent-solubilized Na^+-citrate symporter CitS of *Klebsiella pneumoniae*. Compared to classical hybridoma technology, the *in vitro* selection systems allow a much better control of the structural integrity of the target protein and allow the use of other protein classes in addition to recombinant antibodies. We also compared the selected DARPins to a Fab fragment previously selected by phage display and demonstrate that different epitopes are recognized, unique to each class of binding molecules. Therefore, the use of several classes of binding molecules will make suitable crystal formation and the determination of their 3D structure more likely.

Keywords: Co-crystallization; Designed ankyrin repeat proteins (DARPins); *In vitro* selection; Membrane protein; Multi-angle (static) light scattering (MALS); Na^+-citrate symporter CitS; Phage display; Recombinant antibody Fab fragment; Ribosome display; Protein engineering

1. Introduction

Multitopic membrane proteins, such as channels, transporters or receptors, are involved in many fundamental biological processes and today, the majority of drug targets are integral membrane proteins. Therefore, there is an immediate and growing need for high-resolution structure information to gain detailed insight into the function of membrane proteins at the atomic level.

In the different genomes analyzed to date, 20–30% of all open reading frames encode integral membrane proteins (Wallin and von Heijne, 1998). As of September 2006, only about 100 membrane protein structures[2,3] have been deposited in the Protein Data Bank (Berman et al., 2000), and this even includes all homologs from different species and a number of relatively robust bacterial outer membrane proteins with β-barrel topology. The even smaller number of non-redundant α-helical membrane proteins remains in stark contrast to the about 12,000[4] solved structures of non-redundant[5] soluble proteins. This contrast points out the difficulties in membrane protein structure determination.

* Corresponding author. Fax: +41 44 635 57 12.
E-mail address: plueckthun@bioc.unizh.ch (A. Plückthun).
[1] Present address: Department of Biochemistry, University of Washington, Seattle, WA 98195, USA.

[2] www.mpibp-frankfurt.mpg.de/michel/public/memprotstruct.html
[3] http://blanco.biomol.uci.edu/Membrane_Proteins_xtal.html
[4] http://www.pdb.org/pdb/holdings.do
[5] Proteins with less than 70% identity.

1047-8477/$ - see front matter © 2007 Elsevier Inc. All rights reserved.
doi:10.1016/j.jsb.2007.01.013

1.1. Crystallization of membrane proteins

A major bottleneck in structure determination of membrane proteins is the production of high quality crystals. The difficulties are mainly attributed to the inherent protein flexibility and conformational inhomogeneity of the detergent-solubilized membrane protein–detergent complex. Additionally, the polar surface of those membrane proteins having only very short solvent-exposed loops cannot reach beyond the detergent layer wrapped around the hydrophobic surface, and therefore stable protein–protein contacts essential for crystal packing are not formed.

1.2. Co-crystallization

A relatively new approach to overcome these problems is the co-crystallization of membrane proteins with antibody fragments (reviewed in Hunte and Michel, 2002). For successful co-crystallization a stable complex of an antibody fragment bound to a structural epitope present in the native conformation of the membrane protein is needed. Thereby, the bound antibody fragment reduces the protein flexibility and increases the conformational homogeneity of the membrane protein–detergent complex since it recognizes—ideally—only the native and functional conformation of the membrane protein. This specificity can also be exploited during membrane protein purification to increase the homogeneity of the protein sample (Kleymann et al., 1995). Equally important, the bound antibody fragment provides additional polar surfaces to mediate stable protein–protein contacts for well-ordered crystal packing. However, this specificity comes at a cost: a new binding molecule fulfilling all the above requirements has to be generated for each membrane protein structure to be solved.

Published co-crystals of membrane proteins and antibody fragments include cytochrome *c* oxidase from *Paracoccus denitrificans* (PDB entries 1QLE/1AR1), cytochrome bc1 complex from *Saccharomyces cerevisiae* alone (PDB entries 1EZV/1KB9) and in complex with cytochrome *c* (PDB entry 1KYO), potassium channel KcsA from *Streptomyces lividans* (PDB entries 1K4C/1K4D/1R3I/1R3J/1R3K/1R3L/2BOB/2BOC), and the ClC chloride channel from *Escherichia coli* (PDB entries 1OTS/1OTT/1OTU). Interestingly, in all crystal structures the antibody fragment fills the gap between adjacent membrane proteins in the crystal lattice and mediates important protein–protein interactions for well-ordered packing.

1.3. Monoclonal antibodies

In all published examples the antibody fragments used for co-crystallization were ultimately derived from monoclonal antibodies, and Fab fragments were either produced by proteolysis of the IgG or the antibody fragment genes from hybridomas were cloned and expressed in *E. coli*.

Several fundamental problems are encountered, however, in the generation of monoclonal antibodies with the desired properties from animals. When the solubilized membrane protein is injected into the animals, the detergent is diluted and the further fate of the protein and its conformational integrity cannot be controlled. The use of adjuvants such as mineral oil casts an additional shadow of doubt on maintaining the native structure for a long time. The membrane protein is processed by antigen-presenting cells and at the same time, some molecules need to be bound to IgM on the surface of B-cells, which triggers the antibody response in the animal. It is at least doubtful whether the conformational epitopes would still be intact at this stage, unless the protein is very stable. Subsequent screening of hybridomas for reactivity with the native state of the protein will detect those antibodies that bind to epitopes present in the folded structure—if such antibodies have been elicited at all. However, when producing antibodies against less rigid molecules, e.g. GPCRs, it is highly likely that most binders that do crossreact with the native protein will be directed against exposed N- or C-terminal tails (Niebauer et al., 2006) or extracellular compact domains, rather than that binders recognize the loops connecting the helices in their native conformation. If the protein denatures during the immunization process, many "real" conformational epitopes will be lost and conformation-specific antibodies are not found.

1.4. Our approach

Here, we demonstrate the use of *in vitro* selection methods to overcome the above limitations and we report a fast downstream screening process to efficiently identify suitable binding partners of membrane proteins for co-crystallization. After we showed in a previous study that conformation-specific, high-affinity antibody Fab fragments that bind to the detergent-solubilized Na^+-citrate symporter CitS can be generated by phage display (Röthlisberger et al., 2004), we now expand this approach to another selection system as well as to another class of binding proteins. With the use of a different class of binding proteins the shape of the binding module can be varied and we intended by using different binding molecules to obtain binders to different epitopes. Both factors can lead to different crystal packing, which should clearly increase the chance of crystal formation suitable for high resolution structure determination.

1.5. Recombinant Fab fragments and Designed Ankyrin Repeat Proteins

The two classes of binding proteins investigated and compared here are antibody Fab fragments and Designed Ankyrin Repeat Proteins (DARPins). The heterodimeric Fab fragment (Fig. 1a) consists of the entire light chain (V_L and C_L domains) and the Fd fragment (V_H and C_H domains) of the heavy chain, which—in the format used in this study—are not disulfide-linked to each other (Röthlisberger et al., 2004). The antigen binding site is formed by

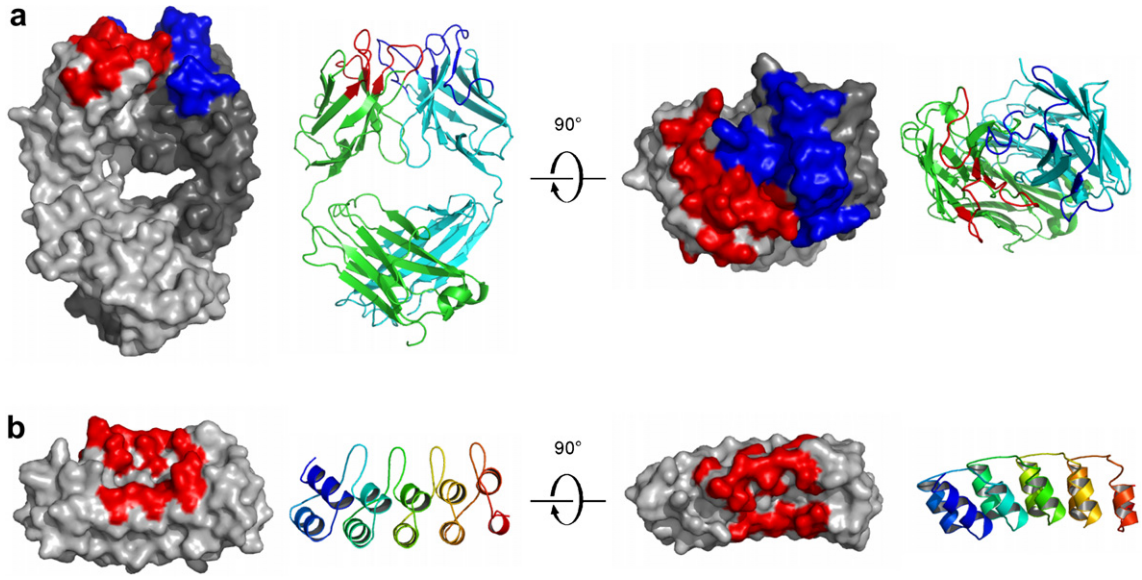

Fig. 1. (a) Surface and corresponding cartoon representation of a Fab fragment. Left, side view where the binding site is on top. The surface of the light chain ($V_L + C_L$) is depicted in light grey and its binding site (CDRs) in red. The corresponding elements of the heavy chain ($V_H + C_H$) are dark grey and the CDRs are depicted in blue. In the cartoon representation, the two chains are colored green (light chain) and cyan (heavy chain). Right, top view on the binding site of the Fab fragment. (b) Surface and corresponding cartoon representation of an N3C consensus DARPin (PDB entry: 1MJ0). The variable positions are colored red in the surface representation. The individual repeats are colored differently in the cartoon picture. Side view (left) and top view (right) on the binding site. Figures were generated with PyMol (DeLano, 2002).

the V_L and V_H domains and is constituted of three loops (complementarity determining regions, CDRs) from each domain, which are highly diverse in sequence and length. We have used a fully synthetic antibody library, based on the original HuCAL consensus design (Knappik et al., 2000), but limiting the library to the most stable and best expressing V_H and V_L frameworks (Ewert et al., 2003), which are randomized in all 6 CDRs and were used in the format of Fab fragments (Röthlisberger et al., 2004). Even though the *in vitro* selection by phage display and the subsequent preparation of milligram quantities of Fab fragments is possible, there are still good reasons to explore alternative frameworks. First, the Fab fragment contains four intramolecular disulfide bonds and can thus not be exposed to reducing conditions that some membrane proteins may require, and second, the preparation of Fab fragments for crystallization trials typically requires five to ten liters of *E. coli* culture. Finally, despite the variety of shapes of antibody binding sites, caused by the length and sequence variation of the CDRs, we have no information on how many different epitopes we actually targeted on a given detergent-solubilized integral membrane protein.

Ankyrin repeat proteins occur in all phyla and mediate important protein–protein interactions in all cell compartments (Bork, 1993). Their modular structure is built from stacked, 33-amino acid repeats, each forming a β-turn followed by two antiparallel α-helices and a loop connecting to the β-turn of the next repeat. Using a combination of sequence and structural alignments, potential interaction residues were identified in the β-turn and first α-helix and were randomized in the library design, while conserved intra- and inter-repeat interactions characteristic for the ankyrin fold were preserved (Fig. 1b) (Binz et al., 2003). Varying numbers of designed ankyrin repeats (typically 2 or 3) were cloned in between specialized N- and C-terminal capping-repeats which seal the hydrophobic core of a stack of the ankyrin repeats that are carrying the potential binding interface. These DARPins are termed N2C and N3C, respectively, denoting their internal repeat numbers. This procedure yielded libraries of DARPins with varying size of randomized interaction surface. Their members have very favorable biophysical properties, very high expression yields (Binz et al., 2003) and have been selected for specific binding to soluble targets before (Binz et al., 2004).

1.6. In vitro selection

The interest in rapid isolation of specific, high-affinity polypeptide binders against a broad range of target molecules lead to the development of different display technologies (Hoogenboom, 2005; Binz et al., 2005). The underlying principle of all these display technologies is the linkage of phenotype and genotype. Thereby, specific binders with desired properties can be enriched from large collections of variants over several consecutive selection cycles. In the present study, phage display and ribosome display were used.

1.7. Phage display

The most widely used display technology is phage display, where the protein (phenotype) is displayed on the sur-

face of a filamentous phage particle while the respective DNA (genotype) is encapsulated inside (Smith and Petrenko, 1997; Hoogenboom, 2002). The power of phage display lies in the robustness of the phage particle, which allows selections to be performed under a wide range of conditions, including the presence of many detergents. A limiting step in phage display, however, is the involvement of *E. coli* transformation, which restricts the diversity of the initial library to 10^9–10^{10} members. In the case of affinity maturation, this *in vivo* step makes the iteration between random mutagenesis, repeated library construction and selection unattractive, as it is very laborious. Furthermore, the *in vivo* amplification of the phage particles can lead to a bias in selection due to growth advantage of certain clones. However, the assembly pathway of filamentous phages allows heterodimers (e.g. Fab fragments) to be displayed on the phage surface. A scheme of the selection cycle is depicted in Fig. 2a.

1.8. Ribosome display

To overcome the limitations caused by the involvement of living cells, ribosome display was developed as a completely *in vitro* display technology (Hanes and Plückthun, 1997). This method relies on the formation of a non-covalent ternary complex of mRNA (genotype), ribosome and nascent polypeptide (phenotype). These complexes are formed during *in vitro* translation, and therefore very large libraries of up to 10^{14} members can be sampled (limited by the amount of cell-free translation extract used and the amount of diverse input DNA). The ease of introducing mutations during the selection cycle by methods such as error-prone PCR or DNA shuffling makes this display technology a very powerful tool for affinity maturation of binding proteins. The relatively low stability of the ternary complex narrows the range of selection conditions, but we show here that selection in detergent for binding to a solu-

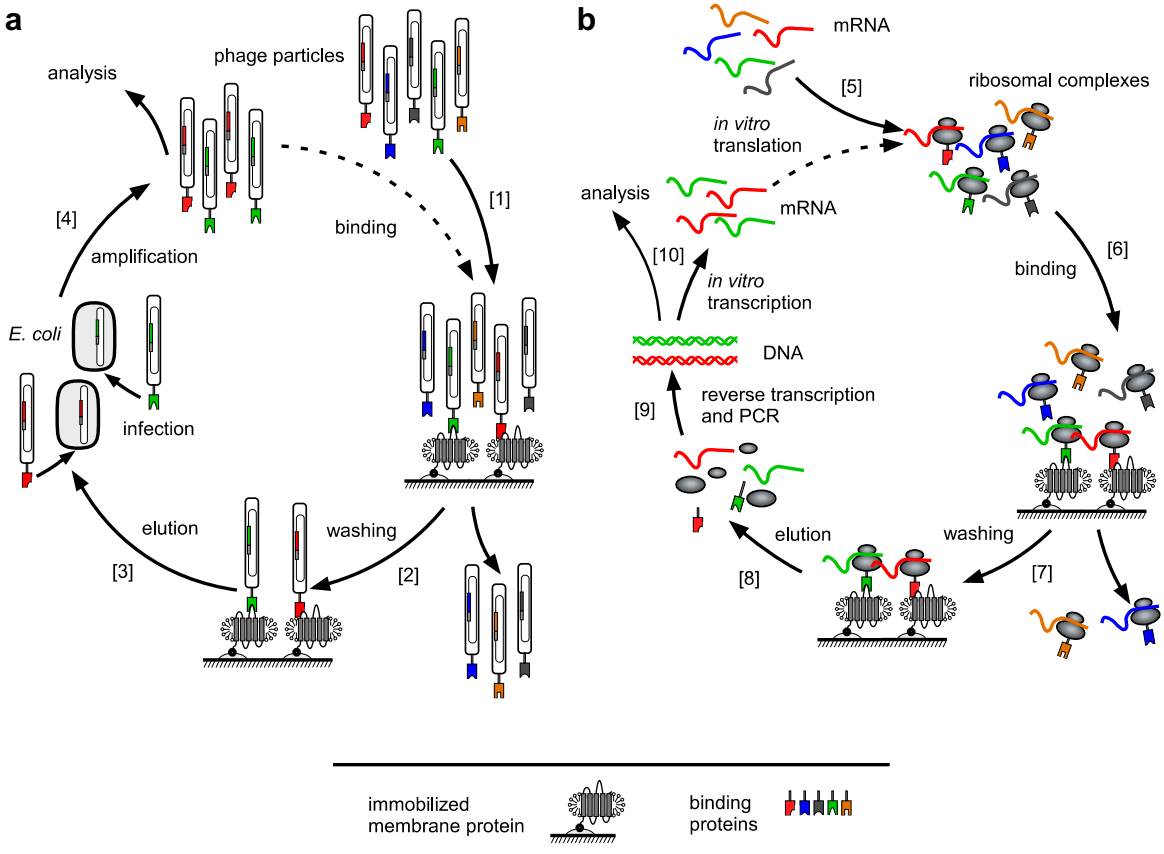

Fig. 2. (a) Schematic representation of a phage display selection cycle. A phage library displaying variants of the protein of interest on the surface while having the respective gene encapsulated inside the phage particle is used for the binding selection on the immobilized target [1]. After formation of the complexes between the binding protein and the membrane protein, unbound phage particles are washed off [2]. The bound phages are eluted from the immobilized target by a pH shift [3] and used for the infection of *E. coli*. Phage particles are amplified [4] and can then be analyzed or used as input for the next selection round. (b) Schematic representation of a ribosome display selection cycle. An mRNA library encoding the proteins of interest without stop codon is translated *in vitro* [5]. After cooling, the translation yields stable ternary complexes of mRNA, ribosomes and nascent polypeptides. These complexes are used for the binding selection on the immobilized target [6]. After binding of the polypeptides to the membrane protein, unbound complexes are washed off [7]. The mRNA of the bound complex is eluted by dissociating the ribosomal complex with EDTA [8]. A reverse transcription reaction followed by PCR yields the genetic information of the selected clones [9]. The amplified genes can then be used as input for the next selection round starting with *in vitro* transcription [10] or cloned into plasmids for analysis.

bilized membrane protein is possible. A scheme of the selection cycle is depicted in Fig. 2b.

1.9. Na^+-citrate symporter CitS as model target

The model system used for this study is the Na^+-citrate symporter CitS from *Klebsiella pneumoniae*, a typical integral membrane protein of the helix-bundle type. CitS has a predicted molecular mass of about 50 kDa and belongs to the family of 2-hydroxy-carboxylate transporters (2HCT)[6] found exclusively in bacteria. Currently, almost 40 members of the 2HCT family are known (Sobczak and Lolkema, 2005). The determined hydropathy profile is highly conserved throughout the family, and it is assumed that all members of the 2HCT family share a common fold. However, no 3D structure is available so far for any member of the 2HCT family. CitS is responsible for citrate uptake during the anaerobic breakdown of citrate in *K. pneumoniae* which ultimately leads to ATP formation. CitS transports the citrate dianion ($Hcit^{2-}$) in symport with two Na^+ ions and one H^+ ion across the membrane. A topology model of CitS was determined using PhoA fusions, site-directed Cys labeling, insertion of reporter proteins, and expression in an *in vitro* translation/insertion system (van Geest and Lolkema, 2000). According to this model, CitS consists of 11 transmembrane segments (TMS) with the N-terminus in the cytoplasm and the C-terminus in the periplasm and relatively short loops connecting the TMS (Fig. 3a). CitS is so far the only member of the 2HCT family that has been purified to homogeneity and functionally reconstituted into proteoliposomes (Pos and Dimroth, 1996). Therefore, it is assumed that CitS is in a functional state when detergent-solubilized. This is not only important for crystallographic studies of the membrane protein but is also crucial for successful *in vitro* selections.

There are certain advantages of using detergent-solubilized membrane proteins as targets for selection over the use of whole cells or reconstituted proteoliposomes. The advantages are the accessibility of both extracellular and intracellular epitopes, the higher monodispersity of the target, and the simplification of the selection procedure. Nevertheless, it must be kept in mind that the detergent may also shield regions (epitopes) of the membrane protein and that the membrane protein might, at least in principle, adopt a non-functional conformation.

[6] *Abbreviations used:* 2HCT, 2-hydroxy-carboxylate transporters; 4NPP, 4-nitrophenyl phosphate; AP, alkaline phosphatase; BAD, biotin acceptor domain; BSA, bovine serum albumin; CDR, complementary determining region; DARPin, Designed Ankyrin Repeat Protein; DDM, *n*-dodecyl-α-D-maltopyranoside; ECL, electrochemiluminescence; HuCAL, human combinatorial antibody library; IMAC, immobilized metal ion affinity chromatography; IPTG, isopropyl-β-D-thiogalactopyranoside; K_D, equilibrium dissociation constant; MALS, multi-angle (static) light scattering; MBP, maltose binding protein; pfu, plaque forming units; SEC, size-exclusion chromatography; TMS, transmembrane segment.

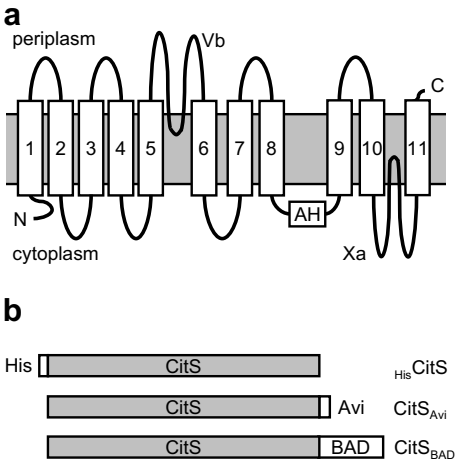

Fig. 3. (a) Simplified topology model of CitS. It contains 11 transmembrane segments, with the N-terminus (N) in the cytoplasm and the C-terminus (C) in the periplasm. The segments Vb and Xa are thought to extend into the membrane. The segment AH is an amphipathic surface helix. This figure is adapted from Sobczak and Lolkema (2005). (b) Schematic representation of the three CitS constructs with corresponding annotation used in this study. The length of the boxes is proportional to the actual length of the protein chain.

2. Materials and methods

2.1. Protein expression and purification

2.1.1. Na^+-citrate symporter CitS from K. pneumoniae

CitS containing an N-terminal His tag. The amino acid sequence M-G-$(H)_{10}$ was fused to the N-terminus of the full length CitS (M83146, aa M1-I446) in the vector pET16b (the expressed protein is termed $_{His}$CitS, Fig. 3b) and expressed in *E. coli* C43(DE3) (Miroux and Walker, 1996) as described by Kästner et al. (2000). *E. coli* C43(DE3) cells were lysed using a French press and CitS was directly solubilized with 2% DDM in 20 mM Tris–HCl, pH 7.5 and 300 mM NaCl. The cleared lysate containing the solubilized CitS was purified by IMAC (Ni^{2+}–NTA, Qiagen). The eluate was further passed over a size-exclusion chromatography column (Superose 6 10/300 GL, GE Healthcare).

Biotinylated CitS. The vector pMalccitSabirA (Kästner et al., 2000) was used to express biotinylated CitS. Biotin ligase BirA was co-expressed from the same plasmid allowing *in vivo* biotinylation. Two constructs were cloned in the vector pMalccitSabirA. One had the biotin acceptor domain (BAD) of oxaloacetate decarboxylase from *K. pneumoniae* (J03885, aa V492-A596) fused to the C-terminus of CitS (the expressed protein is termed $CitS_{BAD}$, Fig. 3b) (Kästner et al., 2000), the other carried an Avi tag (G-L-N-D-I-F-E-A-Q-K-I-E-W-H-E) fused to the C-terminus (the expressed protein is termed $CitS_{Avi}$, Fig. 3b). Both constructs were expressed in *E. coli* DH5α as described by Kästner et al. (2000). Cells were lysed using a French Press and biotinylated CitS was directly solubilized with 2% DDM in 100 mM sodium phosphate, pH 7,

300 mM NaCl and 10% glycerol. Solubilized CitS was purified from the cleared lysate by a monomeric avidin column (Pierce). To remove the free biotin the eluate was passed over a desalting column (NAP-5, GE Healthcare) and subsequently dialyzed twice against 250 buffer volumes each.

2.1.2. Designed Ankyrin Repeat Proteins (DARPins)

Selected DARPins were cloned into pQE30-based (Qiagen) vectors containing an N-terminal M-R-G-S-$(H)_6$ tag. Behind the DARPin coding region, the vector contained either the double stop codon TAA-TGA ($pQE30_{ss}$; the expressed protein is termed $_{His}$DARPin) or a five times repeated myc-tag (M-E-Q-K-L-I-S-E-E-D-L-N-E)$_5$, ($pQE30_{myc5}$; the expressed protein is termed $DARPin_{myc5}$) in front of the double stop codon. Expression of DARPins was performed in *E. coli* XL1-Blue (Stratagene) in dYT medium (5 g NaCl, 10 g yeast extract, 16 g tryptone for 1 liter of media). Expression was induced with 1 mM IPTG (final concentration) at an OD_{600} of 0.6 and continued for 3–4 h at 37 °C.

Cells were resuspended in lysis buffer (40 mM Tris–HCl, pH 7.5, 300 mM NaCl, 20 mM imidazole, 10% glycerol, and 1 mg/ml lysozyme), and passed through a French press, and the cleared lysate was applied to an IMAC column (Ni^{2+}–NTA, Qiagen). Elution fractions were passed over a desalting column (NAP-5, GE Healthcare).

2.2. Ribosome display

The PCR-amplified N3C DARPin DNA-library, described previously (Binz et al., 2004), was transcribed *in vitro* and selection was performed by ribosome display as described by Hanes and Plückthun (1997). MaxiSorp plates (Nunc) were coated with NeutrAvidin (100 µl, 66 nM, overnight at 4 °C), blocked with BSA (200 µl, 0.5%, 1 h at room temperature) and $CitS_{BAD}$ was immobilized via its biotin residue on NeutrAvidin (100 µl, 200 nM $CitS_{BAD}$, 1 h at 4 °C, 10 mM Tris–HCl, pH 7.5, 150 mM NaCl, and 0.05% DDM). Binding and washing buffers (50 mM Tris–HOAc, pH 7.5, 150 mM NaCl, 50 mM $Mg(OAc)_2$, 0.5% BSA, and 0.05% DDM) contained DDM as detergent to keep the membrane protein in its functional conformation. The translation mix, containing the ternary mRNA–ribosome–DARPin complexes, was first pre-panned in two wells (30 and 60 min) against biotinylated MBP, immobilized the same way as $CitS_{BAD}$ to remove DARPins that would bind to the plate for other reasons than recognizing CitS. Subsequently, the translation mix was transferred to the well containing immobilized $CitS_{BAD}$. The library was incubated for 45 min, and the washing time was increased from round to round (15 min total washing time in the first round to 90 min total washing time in the fourth round). After washing, the mRNA was eluted with 100 µl elution buffer (50 mM Tris–HOAc, pH 7.5, 150 mM NaCl, and 25 mM EDTA). A total number of four rounds of ribosome display were performed. The number of PCR cycles after reverse transcription was reduced from round to round from 45 to 35 to 30 to 25, adjusting to the yield due to progressive enrichment of binders in each round.

2.3. Phage display

The generation and characterization of the DARPin-phage library based on SRP-Phage display (Steiner et al., 2006) will be described elsewhere (Steiner et al., manuscript in preparation). All steps of the phage display selection were performed at room temperature. For the first selection cycle 1.6×10^{13} phage particles displaying the DARPin library were incubated for 1 h with 100 nM biotinylated $CitS_{BAD}$ in 2 ml of CitS-buffer (20 mM potassium phosphate, pH 7.0, 500 mM NaCl, 20% glycerol, and 0.1% DDM) containing 0.4% BSA. The phage–antigen complexes were captured on 100 µl streptavidin-coated paramagnetic beads (10 mg/ml, Dynabeads MyOne Streptavidin T1, Dynal) for 20 min. After washing the beads eight times with CitS-buffer the phage particles were eluted with 200 µl of 100 mM Et_3N for 6 min, followed by 200 µl of 100 mM glycine, pH 2, for 10 min. Eluates were neutralized with 100 µl of 1 M Tris–HCl, pH 7, or 18 µl of 2 M Tris–base, respectively, combined and used to infect 5 ml of exponentially growing *E. coli* XL1-Blue cells (Stratagene). After shaking for 1 h at 37 °C cells were plated on dYT agar plates containing 10 µg/ml chloramphenicol and 1% glucose and grown overnight at 37 °C. The cells were scraped off the plates and used to inoculate 15 ml of dYT containing 10 µg/ml chloramphenicol to an initial OD_{600} of 0.1. The culture was incubated at 37 °C with shaking and at an OD_{600} of 0.5 the phage library was rescued by infection with VCSM13 helper phage (Stratagene) at 10^{10} pfu (plaque forming units) per ml (multiplicity of infection ~20). After 1 h at 37 °C, 45 ml of fresh dYT containing 10 µg/ml chloramphenicol, 16.7 µg/ml kanamycin, and 0.27 mM IPTG were added and the culture grown overnight at 30 °C. Cells were removed by centrifugation (5600*g*, 4 °C, 10 min) and the culture supernatant was incubated on ice for 1 h with one-fourth volume of ice-cold PEG/NaCl solution (20% polyethyleneglycol (PEG) 6000, 2.5 M NaCl). The precipitated phage particles were then collected by centrifugation (5600*g*, 4 °C, 15 min) and resuspended in 3 ml of CitS-buffer and used for the second round of selection.

For the subsequent selection rounds, 10^{12} of the amplified phage particles were used as input, beads were washed 12 times with CitS-buffer, phages eluted with 400 µl of 100 mM glycine, pH 2 for 10 min, the eluate neutralized with 36 µl of 2 M Tris–base and used to infect 5 ml of exponentially growing *E. coli* XL1-Blue cells.

Infection was allowed to occur for 1 h at 37 ° C and cells were directly expanded into 50 ml of fresh dYT containing 10 µg/ml chloramphenicol. After 3–4 h at 37 °C, IPTG was added to a final concentration of 0.2 mM and 15 min later VCSM13 helper phage was added to a final concentration of 10^{10} pfu per ml. Cells were grown overnight at 37 °C

without the addition of kanamycin and phage particles harvested as described above.

To determine enrichment of binders, amplified polyclonal phage pools from each selection round were analyzed by phage ELISA as described by Röthlisberger et al. (2004). Further, single clones of round three and four were randomly picked and analyzed by phage ELISA. Positive clones were sequenced and recloned into $pQE30_{ss}$ and $pQE30_{myc5}$ for further analysis.

2.4. Analytical size-exclusion chromatography (SEC)

Size-exclusion chromatography was performed on an Agilent 1100 HPLC system. A molar excess of selected DARPins (30–60 μM) was mixed with $_{His}$CitS (15–30 μM) and incubated in 10 mM Tris–HCl, pH 7.5, 150 mM NaCl, 0.05% DDM for at least 30 min at 10 °C for complex formation. For analysis of the ternary CitS–DARPin–Fab fragment complex, $_{His}$CitS (15 μM) was incubated with both DARPin (30 μM) and Fab fragment (30 μM) for 60 min at 10 °C for complex formation. With a well plate autosampler (Agilent 1100) sample volumes of 75 μl were loaded on a Superdex 200 10/300 GL column (GE Healthcare) with a flow rate of 0.5 ml/min. Fractions of 250 μl were collected with an analytical fraction collector (Agilent 1100).

2.5. Multi-angle light scattering (MALS)

SEC-MALS measurements were performed on an Agilent 1100 HPLC system connected to a tri-angle light scattering detector and a differential refractometer (miniDAWN Tristar and Optilab, respectively; Wyatt Technology, Santa Barbara, CA, USA). Specific refractive index increment (dn/dc) values of 0.186 ml/g (Wen et al., 1996) and 0.133 ml/g (Strop and Brünger, 2005) were used for the protein and the detergent fraction (DDM), respectively. Sample volumes of 200 μl with a CitS protein concentration of 20 μM were injected on a Superose 6 10/300 GL column (GE Healthcare). The data were recorded and processed using the ASTRA V software (Wyatt Technology). To determine the detector delay volumes and normalization coefficients for the MALS detector, a BSA sample (Sigma, A8531) was used as reference. Neither despiking nor a band broadening correction was applied.

2.6. ELISA

Buffers for binding and washing in all ELISA experiments were 10 mM Tris–HCl, pH 7.5, 150 mM NaCl (TBS) supplemented with 0.05% DDM (TBS-D), 0.2% BSA (TBS-B) or both (TBS-DB), if not stated otherwise.

2.6.1. Crude extract ELISA

2.6.1.1. Coating. A MaxiSorp Plate (Nunc) was coated with protein A (Sigma, 100 μl, 10 μg/ml in 100 mM phosphate, pH 7.0, and 150 mM NaCl) for 2 h at 4 °C and blocked for 2 h with 0.2% BSA (Fluka, 200 μl TBS-B) at room temperature. The wells were incubated with 100 μl of a 1:500 dilution of anti-myc antibody (Cell signaling, 9B11) in TBS-B for 1 h at 4 °C.

2.6.1.2. Crude extract from single clones. One milliliter medium (dYT containing 1% glucose and 100 μg/ml ampicillin) was inoculated with single colonies of *E. coli* XL1-Blue, harboring $pQE30_{myc5}$ encoding a selected DARPin, in a 96-deep-well plate and was grown overnight at 37 °C. One milliliter of fresh dYT with 100 μg/ml ampicillin was inoculated with 100 μl of the overnight culture. After incubation for 2 h at 37 °C, expression was induced with IPTG (1 mM final concentration) and continued for 3 h. Cells were harvested, resuspended in 100 μl B-PERII (Pierce) and incubated for 15 min at room temperature with vortexing from time to time. Then, 900 μl TBS-D was added and cell debris was removed by centrifugation.

2.6.1.3. ELISA of lysate. Of each lysate, 100 μl were applied to a well of a MaxiSorp plate containing immobilized anti-myc antibody and incubated for 45 min. After extensive washing with TBS the plate was incubated with 40 nM biotinylated $CitS_{BAD}$ in TBS-DB for 45 min. For competition experiments, 400 nM of the competitor was pre-incubated with biotinylated CitS. After washing with TBS-D, binding was detected with streptavidin-AP conjugate (Roche, 1:1000 dilution in TBS-DB, 30 min at 4 °C) by using di-sodium 4-nitrophenyl phosphate (4NPP, Fluka) as a substrate for AP. The color development was stopped by addition of 3 M NaOH (100 μl) and measured at 405 nm (540 nm reference wavelength) with a plate reader (HTS 7000 Plus, Perkin-Elmer). As negative control the crude extract of an expression culture containing the expression vector without an insert was used.

2.6.2. Competition ELISA with purified proteins

2.6.2.1. Fab directly coated/detection of biotinylated CitS. MaxiSorp plates were coated directly with 250 nM Fab fragment (in TBS, purified as described by Röthlisberger et al. (2004)), incubated for 2 h at 4 °C and blocked with 200 μl TBS-B for 1 h. The plate was then incubated with 40 nM biotinylated $CitS_{BAD}$ in TBS-DB for 45 min. For competition experiments, 400 nM of the competitor was pre-incubated with biotinylated $CitS_{BAD}$. Detection of the bound protein was done as above. In the negative control no Fab fragment was coated.

2.6.2.2. Sandwich ELISA/detection of DARPin via myc tag. Coating of MaxiSorp plates with 250 nM Fab fragment was carried out as described above. Then the plate was incubated with 40 nM $_{His}$CitS in TBS-DB for 45 min. After washing, purified $DARPin_{myc5}$ (50 nM in TBS-DB) was added to the well for 30 min. Detection was performed by incubation with anti-myc antibody (1:1000 dilution in TBS-DB; 45 min at 4 °C) followed by, after washing, goat anti-mouse antibody fused to AP (Sigma, 1:2000 in

TBS-DB; 30 min at 4 °C). Color development and measurements were carried out as above. In negative controls there was either no Fab fragment coated or the Fab fragment was incubated with buffer only instead of $_{His}$CitS.

2.7. Determination of dissociation constants by equilibrium titration

To determine the dissociation constants of the DARPins electrochemiluminescence (ECL)-based equilibrium titration was performed using the ECL-detection system of BioVeris (Witney, Oxfordshire). Streptavidin-coupled paramagnetic beads were coated with $CitS_{Avi}$, and bound $DARPin_{myc5}$ was detected by an anti myc-tag antibody (Cell signaling, 9B11), which in turn was detected with an anti-mouse IgG labeled with the BV-tag (BioVeris). The BV-tag consists of a tris(2,2′-bipyridine)ruthenium(II) complex, covalently linked to the protein, that emits light when electrooxidized in the presence of aliphatic amines, such as tri-*n*-propylamine (Miao et al., 2002). The amount of DARPin bound to immobilized $CitS_{Avi}$ was measured as a function of competing $_{His}$CitS in solution. The assay buffer used for all dilution, wash and assay steps was 10 mM Tris–HCl, pH 7.5, 150 mM NaCl containing 0.05% DDM and 0.2% BSA (TBS-DB). Coating of the beads with $CitS_{Avi}$ was performed at 4 °C, all other steps at room temperature.

2.7.1. Detection mix

A suspension of 40 μg/ml streptavidin-coupled paramagnetic beads (Dynabeads MyOne Streptavidin T1, Dynal biotech) was washed and then incubated with 2.5 nM $CitS_{Avi}$ for 45 min under vigorous shaking. The beads were washed to remove free $CitS_{Avi}$. Subsequently, anti-myc antibody (Cell signaling, 9B11) as well as anti-mouse IgG antibody carrying the BV-tag (BioVeris) were added, each at 1:200 dilutions.

2.7.2. Assay

Dilutions of $_{His}$CitS in the range from 50 pM to 2 μM were mixed with 5 nM of $DARPin_{myc5}$ and 15 μl of detection mix to yield a total assay volume of 150 μl. Under vigorous shaking, the samples were incubated at room temperature for at least 4 h. Subsequently, ECL signals were detected in 96-well format with a M1M analyzer (BioVeris Corporation). The plate was incubated for 10 min in the M1M analyzer under shaking.

2.7.3. Data analysis

The DARPin can either bind to immobilized $CitS_{Avi}$ on the beads or to free $_{His}$CitS in solution. This can be described by two equilibria, assuming a 1:1 interaction Eq. (1).

$$C + A \rightleftharpoons CA \text{ and } C_b + A \rightleftharpoons C_bA \quad (1)$$

where C is the His-tagged CitS ($_{His}$CitS), A is the myc-tagged DARPin ($DARPin_{myc5}$) and C_b is the bound Avi-tagged CitS ($CitS_{Avi}$) present on the beads.

Assuming the same dissociation constant K_D for both equilibria and that each CitS monomer interacts with one DARPin independently, we derived Eq. (2) from the basic equations that describe the two equilibria Eq. (1) (see Online Supplement for derivation)

$$ECL = \frac{Const.}{2\left(\frac{[C]_t}{[C_b]_t}+1\right)}\left\{([A]_t + [C]_t + [C_b]_t + K_D) - \sqrt{([A]_t + [C]_t + [C_b]_t + K_D)^2 - 4\left(\frac{[C]_t}{[C_b]_t}+1\right)[C_b]_t[A]_t}\right\} + BG \quad (2)$$

where $[C]_t$ is the total concentration of added $_{His}$CitS, $[C_b]_t$ is the total amount of $CitS_{Avi}$ present on the beads (given as a molar concentration in the assay), $[A]_t$ is the total concentration of added $DARPin_{myc5}$, *Const.* is a proportionality constant that correlates the concentration of C_bA to the measured signal, *ECL* is the measured signal and *BG* is the background signal.

The parameters K_D, $[A]_t$, *Const.* and *BG* were fitted to the data using Eq. (2) with Prism 4 (GraphPad software Inc.). Measurements where carried out in duplicates. In order to be able to compare the different DARPins in one plot the ECL signals were normalized between 0 and 1 according to the fitted curves.

3. Results

We describe here the selection of Designed Ankyrin Repeat Proteins (DARPins) by ribosome display and phage display for binding to detergent-solubilized Na^+-citrate symporter CitS. We adapted several methods to be able to quickly and efficiently screen and characterize the binding proteins. Furthermore, we compare the obtained DARPins to a previously selected HuCAL Fab fragment binding to CitS.

We used CitS immobilized via a biotinylation tag as the target for selection. Both constructs (see Fig. 3b), CitS carrying a C-terminal BAD domain ($CitS_{BAD}$) or an Avi tag ($CitS_{Avi}$), were functional in *E. coli*, as determined with an *in vivo* assay based on growth of transformed *E. coli* on Simmons citrate agar (Kästner et al., 2000). We previously found the biotin–NeutrAvidin/streptavidin interaction to be the most robust linkage for immobilizing detergent-solubilized membrane proteins. By contrast, the binding of many other tags to their cognate antibodies is weakened by detergent. The immobilization via the His tag to immobilized Ni^{2+}–NTA is much too weak (Lata and Piehler, 2005) and further destabilized by the detergent-containing buffer (Ott and Plückthun, unpublished experiments). Even though we cannot prove directly that CitS is active in detergent, it can be reconstituted into lipid vesicles from the detergent mixture (Pos and Dimroth,

1996). Therefore, it is a reasonable assumption that it is in a state very close or identical to that in the native bilayer.

3.1. Ribosome display selection against CitS

For ribosome display, biotinylated CitS ($CitS_{BAD}$) was immobilized to microtiter plates coated with NeutrAvidin. The selected DARPin pools of all four rounds of ribosome display were subcloned into the expression vector pQE_{myc5}. After transformation, randomly picked single clones were sequenced to estimate the diversity of the pools. None of the 12 sequenced clones of each round carried the same DARPin. This result indicates that the pools are still diverse and that a wide variety of different binding molecules can be obtained. A strong enrichment of binding signal was observed after the fourth selection round by ELISA of the pool (data not shown).

Single clones (70) of the fourth round were further analyzed by crude extract ELISA. To quickly and reliably screen for positive clones, the selected DARPins were immobilized on the plate via the myc-tag, and the binding of solubilized membrane protein was detected. In this setup, the membrane protein was exposed to a minimum of washing and incubation steps (see Section 2). About 35% of the clones (25 out of 70 initially screened clones) showed a binding signal to $CitS_{BAD}$. To test whether binding was really specific for the membrane protein, free $_{His}$CitS, carrying no biotinylation tag, was used as competitor. For around 40% of the positive clones (10 out of 70 initially screened clones) the binding signal was decreased or even reduced to the background level upon addition of excess competitor $_{His}$CitS, consistent with specific binding. None of the sequenced CitS-specific DARPins showed the same sequence, indicating that even more DARPins may be found with further screening.

About half of the clones showing binding signal (15 of 25 clones) were false-positive. For biotinylation, BAD (biotin acceptor domain from oxaloacetate decarboxylase (Schwarz et al., 1988), about 100 amino acids long) was fused to CitS, and the presence of an additional folded domain in the selection procedure has apparently also resulted in—unwanted—selection of some DARPins specific for the BAD domain. Nevertheless, as determined by ELISA of the selection pools (data not shown), a greater percentage of non-CitS binders that became enriched is due to truly unspecific binding and only a smaller percentage shows binding to BAD.

3.2. Phage display selection against CitS

The phage display library used for the selection has a functional diversity of 1.1×10^{10} (Steiner et al, in preparation). Since DARPins are normally cytoplasmic proteins that fold very fast and are very stable, they are not compatible with standard phage display systems, and they have to be directed to the *E. coli* signal recognition particle (SRP) translocation pathway by the use of an appropriate signal sequence (Steiner et al., 2006). With the appropriate phagemid, phage display is then at least as efficient as with libraries of other proteins and peptides.

Since unspecific binding was observed in ribosome display, where CitS had been immobilized to a microtiter plate, the selection procedure in phage display was carried out by first letting solubilized $CitS_{BAD}$ bind to DARPin-carrying phages in solution and then capturing the complexes with streptavidin-coated beads. This "solution panning" requires larger amounts of $CitS_{BAD}$, but has the advantage of reducing unspecific interaction with the plate surface.

Four rounds of selection on solubilized $CitS_{BAD}$ in solution, followed by capturing of the antigen with streptavidin-coated paramagnetic beads, were performed. An enrichment of the binding signal was observed already after the second selection round. After the third and fourth round of selection, 62 clones each were screened in phage ELISA format for binding to immobilized $CitS_{BAD}$ in the absence or presence of an excess of soluble $_{His}$CitS as competitor. Eighty-nine percent of the clones (110 out of 124 initially screened clones) showed a binding signal on immobilized $CitS_{BAD}$, of which 17% (19 clones) could be inhibited by the addition of competitor ($_{His}$CitS). Sequencing revealed 11 different sequences (around 9% of initially screened clones).

Compared to panning on microtiter plates, solution panning lead to a reduction of unspecific binders, but the percentage of—undesired—BAD-specific binders was increased (data not shown). While in the ribosome display experiment described above the membrane protein was immobilized via its biotin tag prior to adding the ribosomal complex (thereby making the BAD domain less accessible), in phage display the selection was carried out in solution and the BAD domain was fully accessible. To increase the fraction of binders specific for CitS itself, a prepanning step on the BAD domain alone can be included, or a CitS version without BAD domain (e.g. carrying an Avi tag) can be used in the future. It should be emphasized that either immobilization strategy, solution panning or plate panning, can of course be used with either display technology, phage display or ribosome display.

3.3. Size-exclusion chromatography (SEC) of complexes

By using SEC, the formation of stable complexes in solution can be monitored directly. Additionally, the potential aggregation tendency of any selected binder can be assessed, usually an undesired property for co-crystallization. Furthermore, the use of purified $_{His}$DARPins for the subsequent analysis eliminates possible influences of the phage or crude lysate on the binding and solubility behavior.

The subset of different DARPins chosen based on efficient inhibition of ELISA signals by soluble $_{His}$CitS and on sequencing (10 from ribosome display and 11 from phage display, as described above) was further analyzed

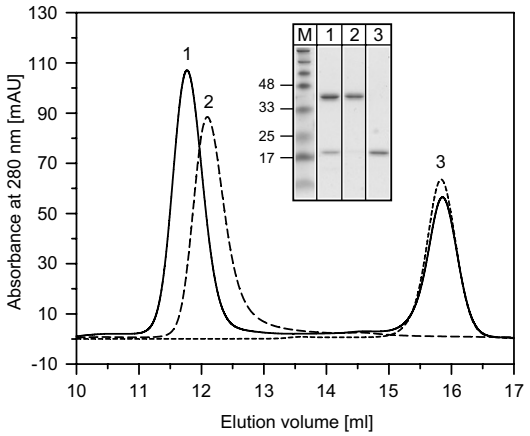

Fig. 4. Superposition of size-exclusion chromatography (SEC) elution profiles. Free CitS (dashed line, peak 2), free DARPin cp34h_15 (short dashed line, peak 3) and CitS mixed with excess DARPin cp34h_15 (solid line, peak 1) were loaded on a Superdex 200 column. The elution peak of the CitS–DARPin (peak 1) complex is shifted to smaller elution volume (i.e. bigger molecular size) compared to free CitS (peak 2). The Coomassie brilliant blue-stained SDS–polyacrylamide gel of the corresponding peak fractions is shown in the inset. The DARPin has a molar mass of 18 kDa, $_{His}$CitS of 50 kDa, but runs on SDS–PAGE at about 40 kDa.

Table 1
Properties of selected DARPin in comparison to a selected Fab fragment

	cr34_8C4	cp34_15	cp34_16	f3p4[a]
Protein class	DARPin	DARPin	DARPin	Fab fragment
Selection method	Ribosome display	Phage display	Phage display	Phage display
Molar mass (kDa)	18.2	18.2	18.4	47.9
p*I*	5.1	5.3	4.9	4.8
Affinity (nM)	2.5 ± 0.6[b]	5.4 ± 1.9[b]	1.3 ± 0.3[b]	4 ± 2[c]
Yield[d] (mg/liter)	>30[e]	>75[e]	>20[e]	3

[a] Previously described by Röthlisberger et al. (2004).
[b] Equilibrium titration (BioVeris).
[c] Competition BIAcore.
[d] Yield of purified protein from a 1 liter *E. coli* shake flask culture.
[e] IMAC column was strongly overloaded, therefore the yield is greatly underestimated.

by SEC. A molar excess of purified DARPin was mixed with $_{His}$CitS and loaded on a SEC column. Since the binding stoichiometry of CitS–DARPin complexes was not known, the DARPin was used in excess (relative to the subunit concentration of the presumed dimeric CitS) and at micromolar concentrations to allow complex formation of all CitS molecules. Complex formation is indicated by a shift of the CitS elution peak to smaller elution volume (i.e. bigger molecular size) relative to the uncomplexed $_{His}$CitS. SDS–PAGE analysis of the corresponding peak fraction of the presumed complex showed that the fraction contained both CitS and DARPin (Fig. 4).

Only a few of the initially screened binders (1 out of the 70 from ribosome display and 2 out of 124 from phage display) fulfilled the stringent criteria of forming complexes that showed a clear shift in elution volume and having only one distinct elution peak (i.e. no aggregation or residual uncomplexed CitS). We further characterized this one DARPin selected by ribosome display (cr34_8C4) and the two selected by phage display (cp34h_15 and cp34h_16) in more detail and compared them to each other and to the Fab fragment (f3p4) that had been previously selected as binder to solubilized CitS by phage display (Röthlisberger et al., 2004). An overview of the properties of the characterized binders is given in Table 1.

3.4. SEC-MALS of CitS and complexes

The SEC system was further connected to a multi-angle (static) light scattering (MALS) detector and a differential refractive index detector (dRI). These two detectors together with the UV-detector allow the direct comparison of the corresponding molar masses of CitS alone and the complexes. The scattered light (the Rayleigh ratio $R_{(\theta)}$) measured by the MALS-detector is directly proportional to the product of the weight-average molar mass and the solute concentration (Wyatt, 1993; Wen et al., 1996; Folta-Stogniew and Williams, 1999). Either a UV-detector or a dRI-detector alone can be used to calculate online the concentration of a soluble, non-conjugated protein. In contrast, as membrane proteins consist of a protein core surrounded by a detergent fraction, both UV-detector and dRI-detector are required to calculate molar masses. If the UV-extinction coefficient and the differential refractive index increment (dn/dc) of the protein and the detergent are known, the molar masses of the protein fraction and the detergent fraction can be determined. In case of CitS, we calculated the UV-extinction coefficient based on the amino acid sequence and assumed a dn/dc of 0.186 g/ml (Wen et al., 1996) for the protein fraction and a dn/dc of 0.133 (Strop and Brünger, 2005) for the detergent fraction (DDM). In our buffer, we detect for CitS a monodisperse peak with a molar mass of the protein fraction (protein without detergent) of 105–115 kDa (Fig. 5a). This molar mass corresponds to the CitS dimer (theoretical molar mass of 100 kDa including His tag). The dimeric state of CitS is in agreement with single molecule fluorescence spectroscopy experiments (Kästner et al., 2003).

In the case of the CitS complexes, we first have to assume an extinction coefficient, as we do not know the binding stoichiometry initially. In the case of the CitS–Fab fragment complex (molar masses of both are about 50 kDa) only a 2:1 (CitS:Fab fragment) stoichiometry gives a meaningful result. The molar mass of the protein fraction is then determined to be 155–165 kDa (Fig. 5b). For the smaller CitS–DARPin complexes, however, the assumption of different binding stoichiometries (2:2 CitS:DARPin or 2:1 CitS:DARPin) and therefore different extinction coefficients does not lead to an unequivocal distinction and therefore both stoichiometries remain possible.

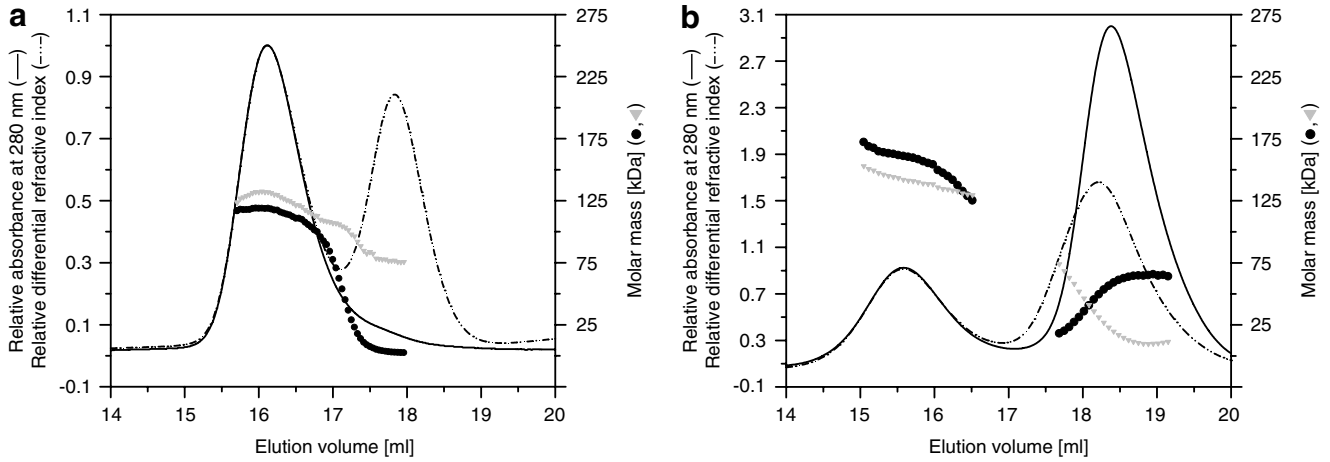

Fig. 5. (a) Characterization of CitS with size-exclusion chromatography combined with multi-angle light scattering (SEC-MALS). CitS (200 μl, 20 μM) was loaded on a Superose 6 column. Only the protein fraction of CitS contributes to the UV-A_{280} signal (solid line), whereas both the protein and the detergent fraction contribute to the differential refractive index signal (dashed-dotted line). The membrane protein–detergent complex elutes at 16.1 ml. The molar mass of the protein fraction is calculated to be 105–115 kDa (filled circles), which corresponds to a CitS dimer (theoretical molar mass of 100 kDa). With 125–140 kDa, the detergent fraction (grey triangles) has a slightly larger molar mass. The empty detergent (DDM) micelles, originating from concentration of the sample prior to injection, elute at 17.9 ml and have a calculated molar mass of 74–76 kDa and are characterized by a peak in refractive index, but not in UV-A_{280}. (b) Characterization of CitS–Fab fragment complex with size-exclusion chromatography combined with multi-angle light scattering (SEC-MALS). CitS (20 μM) was incubated with excess of Fab fragment (f3p4, 60 μM) complex for 1 h at 4 °C and loaded (200 μl) on a Superose 6 column. The UV-A_{280} signal is depicted as solid line, the differential refractive index increment as dashed-dotted line. The molar mass of the protein fraction of the CitS–Fab fragment–detergent complex is 155–165 kDa (filled circles). This corresponds to the molar mass of one Fab fragment bound to a CitS dimer (theoretical molar mass 150 kDa). The molar mass of the detergent fraction is indicated with grey triangles. The elution peak of the excess of Fab fragment (UV-A_{280} at 18.5 ml, and filled circles for the molar mass) superimposes with the empty detergent micelle (peak in differential refractive index at 17.9 ml and grey triangles for the molar mass).

Nevertheless, we can clearly demonstrate a larger molar mass of the complexes by the increased Rayleigh ratio $R_{(\theta)}$, compared to CitS alone.

3.5. Competition ELISA

$DARPins_{myc5}$ were immobilized via the myc-tag on a MaxiSorp plate coated with anti-myc antibody and the binding of biotinylated $CitS_{BAD}$ was competed with a 10-fold excess of either non-biotinylated $_{His}$CitS to confirm specificity, or a 10-fold excess of another $_{His}$DARPin or Fab fragment (f3p4) to test whether they recognize identical or overlapping binding epitopes.

The binding signal of all DARPins can be reduced to background levels with an excess of free $_{His}$CitS (Fig. 6a). This finding demonstrates that the characterized DARPins bind specifically to solubilized CitS, confirming the results from the first ELISA screens. All analyzed DARPins do recognize the same or overlapping epitopes, as the binding of one DARPin to CitS can be inhibited with an excess of another free DARPin. However, the Fab fragment (f3p4) seems to recognize a different epitope, as it does not significantly reduce the binding signal of the DARPins.

To further confirm this finding, the setup of the ELISA was inverted. The Fab fragment (f3p4) was directly coated on the plate and its binding to $CitS_{BAD}$ alone or to $CitS_{BAD}$ pre-incubated with either non-biotinylated $_{His}$CitS, free Fab fragment (f3p4) or free $_{His}$DARPin was compared. The binding signal could be fully competed with excess of $_{His}$CitS or Fab fragment (f3p4) but not with any of the selected DARPin. These results strongly indicate that the two scaffolds do indeed recognize different, non-overlapping epitopes (Fig. 6b).

3.6. Sandwich complex with Fab, CitS and DARPin

To determine if the selected DARPins and the Fab fragment (f3p4) can bind simultaneously to CitS and can therefore form a ternary complex, we performed a sandwich ELISA. In this setup, the Fab fragment (f3p4) was immobilized directly on the plate and subsequently incubated with $_{His}$CitS and $DARPin_{myc5}$. The binding of the $DARPin_{myc5}$ to the $_{His}$CitS–Fab complex was detected. In the negative controls, the Fab fragment was either incubated with BSA instead of $_{His}$CitS or BSA was coated on the well instead of the Fab fragment. The binding signal of the DARPin to $_{His}$CitS-Fab complex is significantly higher than that of the negative controls (Fig. 6c), and therefore the ternary complex seems to be formed for all DARPins.

If the DARPin, the Fab fragment and CitS are able to form a ternary complex, an additional shift in size-exclusion chromatography should be observed. The DARPin (cp34h_15), the Fab fragment (f3p4) and $_{His}$CitS were incubated for 1 h at 10 °C and the mixture was injected on a SEC column. The elution profile of the putative ternary complex is indeed shifted, compared to the binary complex of CitS and DARPin (Fig. 7) and the SDS–PAGE analysis

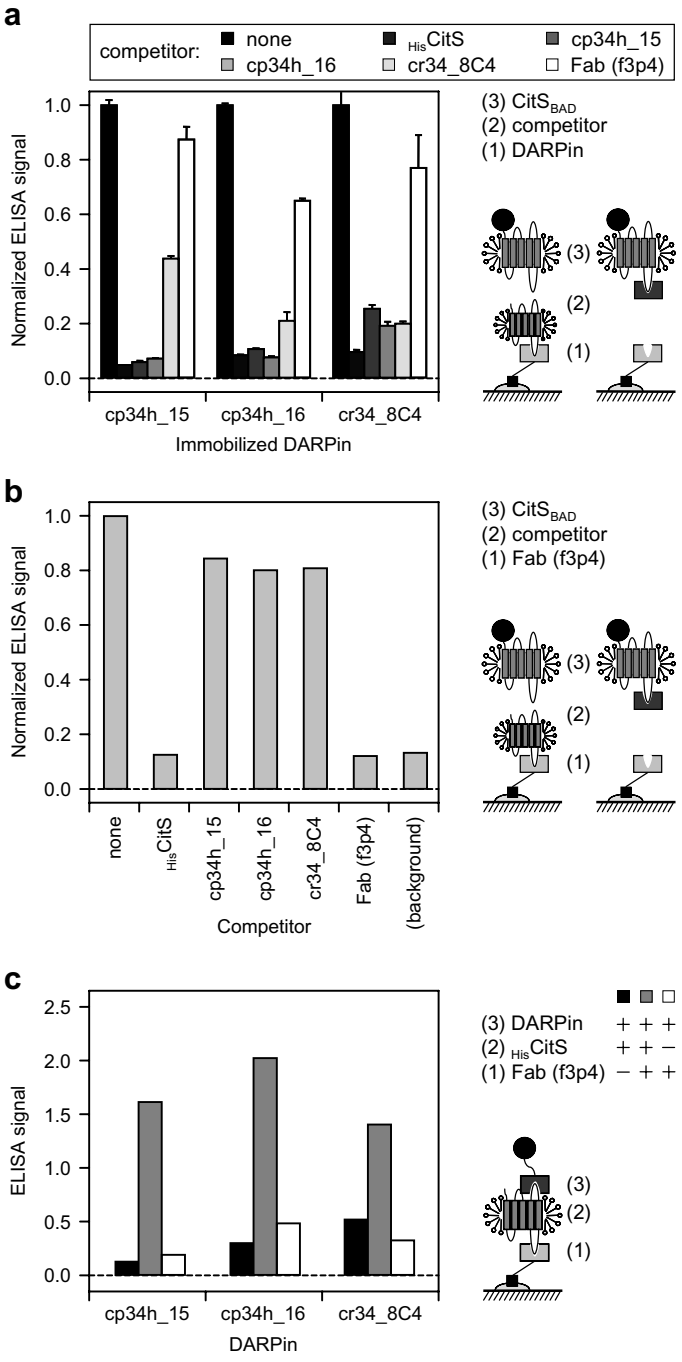

Fig. 6. (a) Competition ELISA assay of DARPins and Fab fragment reveals whether the binding molecules recognize the same or different epitopes. $DARPins_{myc5}$ (40 nM) were immobilized and binding to $CitS_{BAD}$ (40 nM) was detected. The binding signal without competition was normalized to 1. Competition with excess of $_{His}$DARPin and Fab fragment (all 400 nM) was examined. DARPins compete with each other for the same epitope, as the binding signal is clearly reduced. In contrast, there is no significant decrease when competed with the Fab fragment (f3p4). Competition with $_{His}$CitS (400 nM) is included as a control for specific binding. (b) Competition ELISA assay. The binding of $CitS_{BAD}$ to the immobilized Fab fragment (f3p4, 250 nM) was competed with an excess of either non-biotinylated $_{His}$CitS, Fab fragment or $_{His}$DARPins (all 400 nM). Both $_{His}$CitS and Fab fragment reduce the binding signal to background levels, which demonstrates the specificity of the binding. All DARPins do not significantly influence the binding, indicating that they bind to another epitope than the Fab fragment. (c) Sandwich ELISA assay. The Fab fragment f3p4 was immobilized on the plate (250 nM) and incubated with $_{His}$CitS (40 nM). The amount of $DARPin_{myc5}$ that binds was detected via the myc-tag. Binding signal of $DARPin_{myc5}$ to the CitS–Fab complex (grey), binding to $_{His}$CitS on a BSA-coated plate (black) and to Fab fragment without $_{His}$CitS (white).

of the elution peak reveal the presence of CitS, DARPin and Fab fragment in this peak fraction. Beside the main peak of the ternary complex, an additional peak appears, indicating higher aggregates. This peak shows the same SDS–PAGE band pattern as the main peak (data not shown).

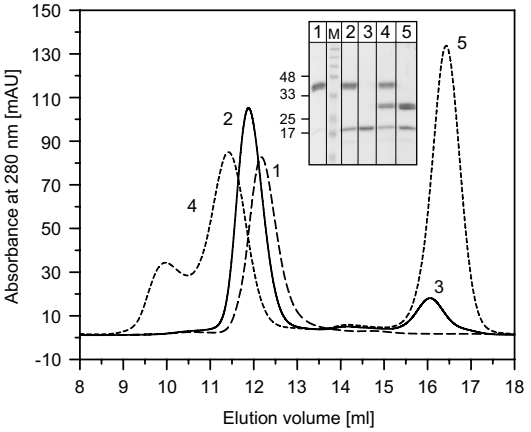

Fig. 7. Characterization of CitS–DARPin–Fab complex with size-exclusion chromatography. Elution profile of $_{His}$CitS (dashed line, peak 1), $_{His}$CitS mixed with an excess of DARPin cp34h_15 (solid line, peaks 2 and 3) and $_{His}$CitS mixed with an excess of both DARPin cp34h_15 and Fab fragment f3p4 (short dashed line, peaks 4 and 5). The Coomassie brilliant blue-stained SDS–polyacrylamide gel of the corresponding peak fractions is shown in the insert. The DARPin has a molar mass of 18 kDa, the two chains of the Fab fragment of 23 and 25 kDa, $_{His}$CitS of 50 kDa (but runs on SDS–PAGE at about 40 kDa). The Fab fragment elutes with some retardation from this size-exclusion column (Röthlisberger et al., 2004).

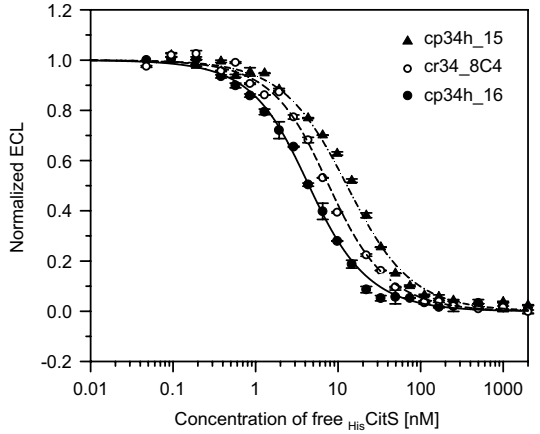

Fig. 8. Determination of dissociation constants by equilibrium titration in solution. Titration curves of three DARPins incubated with varying concentrations of $_{His}$CitS (0.05 nM to 2 μM). The amount of DARPin$_{myc5}$ that still binds to CitS$_{Avi}$ immobilized on beads is measured by ECL. Cp34h_16 (filled circles), cr34_8C4 (open circles) and cp34h_15 (filled triangles) show a K_D of about 1.3, 2.5, and 5.4 nM, respectively. The fits are according to Eq. (2).

3.7. Affinity determination by equilibrium titration

After demonstrating the specificity of the selected binder in ELISA experiments and the formation of well defined stable complexes in SEC experiments, the binding affinity of the selected DARPins was assessed by equilibrium titration in solution. This method is suitable for determination of dissociation constants (K_D) in a high-throughput format needed for the fast characterization of larger number of binding proteins (Haenel et al., 2005). Constant amounts of DARPin were incubated with varying amounts of $_{His}$CitS as competitor and the detection mix containing CitS$_{Avi}$ coated on magnetic streptavidin beads and two detection antibodies. The binding signal was detected with a BioVeris workstation. The binding curves reveal dissociation constants (K_D) in the low nanomolar range (1–6 nM) for all DARPins (Fig. 8) tested. Even though CitS is a dimer, the data could be fitted well to a simple model (Eq. (2), see Section 2), where each CitS monomer interacts with one DARPin independently. We cannot exclude a more complicated model, where the two binding sites may influence each other, but we can get a reasonable fit to the binding data already for the simple model.

4. Discussion

Future efforts in the structure determination of membrane proteins will have to be focused on the development of new tools and technologies to expedite the process and increase the likelihood of success. Co-crystallization with binding molecules is a promising approach to achieve crystals suitable for high resolution structure determination. However, the generation of new monoclonal antibody fragments by the classical hybridoma approach for each membrane protein is not only a costly and time-consuming procedure but may not even be particularly promising for helical, multi-spanning flexible membrane proteins. The fundamental obstacle is that the conformational integrity of the detergent-solubilized proteins cannot be controlled once injected into an animal. In contrast, the use of synthetic libraries and *in vitro* selection technologies, such as phage display and ribosome display, provide a powerful tool to generate such binding molecules in a fast and reliable way. Furthermore, selection conditions can be adapted to the need of the target protein as the binding step is performed *in vitro*.

Since the Na^+-citrate symporter CitS is a multi-spanning integral membrane protein with relatively short loops, it serves us as a model system for selecting such binding proteins for stabilization and mediating additional crystal contacts. By carrying out the comparative analysis of different selections systems and classes of binding molecules, we could demonstrate that both selection technologies (ribosome display and phage display) can be applied. To generate binding molecules against as many epitopes as possible several scaffolds (e.g. DARPin and Fab fragment) need to be considered simultaneously.

4.1. DARPins vs. Fab fragments

Although both scaffolds (DARPin and Fab fragment) compared in this study are used in nature for specific and high affinity binding interactions, they have quite different properties, each with its advantages and disadvantages. DARPins can be obtained in extremely high yields (up to 200 mg soluble protein per liter *E. coli* shake flask culture), and they tolerate the presence of reducing agents, as

DARPins do not contain any disulfide bonds or free cysteines. The Fab fragments are about 2.5 times the size of DARPins (50 vs. 18 kDa, Fig. 1) and may present a larger hydrophilic surface for stable protein–protein contacts in the crystal. As the binding site resides at the tip of the Fab fragment, compared to a more shallow binding groove along the DARPin, the Fab fragment can protrude further out and potentially leave more space in the crystal for the membrane bound detergent molecules. However, Fab fragments are built from several domains and therefore display more conformational flexibility than the very rigid and stable ankyrin fold. Most importantly, the binding surface is realized completely differently in the two scaffolds. In DARPins, the binding residues reside in stable secondary structure elements and short β-turns, displaying an ideal shape complementary to folded proteins (Fig. 1), whilst being less suitable to bind unstructured peptides. Therefore, both the molecular design and the *in vitro* selection strategy significantly increase the likelihood of obtaining binders against structural epitopes, rather than unstructured tails. In antibodies, flexible loops with varying size form the binding site to ensure the recognition of a wide range of antigens (such as small molecules, peptides or entire proteins). Therefore, completely independent epitopes can be bound by the two scaffolds (as shown in this study), which can and should be exploited for the *in vitro* generation of binding molecules for co-crystallization.

4.2. Ribosome display vs. phage display

This study demonstrates that both phage display and ribosome display are well suited for *in vitro* selection of binding proteins, even in detergent-containing buffers needed for membrane proteins. Phage display, when carried out in solution, showed higher enrichment of binding molecules after four cycles than ribosome display, which was carried out on immobilized membrane protein in the example described here. However, fast enrichment obtained by very stringent selection conditions can lead to lower diversity within the selected binding molecule population, with the caveat that none of the selected binders may have the desired properties needed for co-crystallization. It is therefore important to find the right balance between the number of selection cycles, the stringency of washing steps and the selection system applied. We would like to reemphasize that both ribosome display and phage display can be carried out in solution or on surfaces (see next section).

4.3. Solution panning vs. surface panning

The—unwanted—selection of BAD-specific DARPins shows how the applied immobilization method can influence the outcome of a selection. First, the use of a fusion protein for selection always bears a risk to generate unwanted binders against the fusion partner. However, if a fusion partner is needed because of solubility or stability issues, fusion proteins should be changed between subsequent selection rounds or a prepanning step on the fusion partner should be included. Second, the immobilization of the antigen prior to the panning step can mask potential binding epitopes. The use of a longer linker between protein and immobilization tag or a mixture of antigens which carry the immobilization tag either at the N- or the C-terminus can circumvent such an event.

4.4. Workflow

We established an efficient workflow for the characterization of potential binding proteins that allows rapid identification of binding molecules suitable for co-crystallization (Table 2). First, we had to evaluate and adapt the

Table 2
Overview of the workflow for the screening and characterization of DARPins after the selection

Step	Ribosome display	Phage display	Comments
Pool ELISA	Fourth round (then 70 clones were picked for screening)	Third and fourth round (then 62 clones of each round were picked for screening)	Defines of which round the analysis of single clones is worthwhile
Crude extract ELISA	35% (25)[a]	n.d.[b]	Clones that show binding
Phage ELISA	n.a.[c]	89% (110)[a]	Clones that show binding
Competition ELISA	14% (10)	17% (19)	Competition with free CitS indicates specificity
Sequencing	14% (10)	9% (11)	Identification of non-identical DARPin sequences
SEC	1.4% (1)	1.6% (2)	Formation of a well defined, stable complex in solution, no aggregation even at high concentration
Affinity	2.5 nM	1.3 nM, 5.4 nM	Equilibrium titration for affinity determination; ranking of binders according to the K_D
Competition ELISA	All recognize overlapping epitopes as all are competable		Competition with free DARPins distinguishes overlapping or different epitopes

Binding proteins that pass each screening step are given as percentage of the number of initially screened binders.
[a] For this study, initially 70 single clones of ribosome selection and 124 of phage display selection were screened (then 62 from round 3 and 62 from round 4). In parentheses the absolute number of clones is given.
[b] n.d., not done.
[c] n.a., not applicable.

methods, with respect to reliability to work under conditions required for membrane proteins. Then, we chose a format to screen and fully characterize the binding molecules with the least effort and time consumption. As first screen, single clone crude extract ELISA is used. This assay must distinguish specific binding to the membrane protein from binding to fusion partners, tags, streptavidin or BSA used for blocking. The most straightforward test for all of the requirements above in a single experiment is the competition of the binding signal with the membrane protein itself. This assay also tests whether binding occurs only to a surface-bound form of the membrane protein, which would indicate that binding is most probable to a non-native state of the membrane protein. As second screen, SEC is performed using purified DARPins to check for complex formation in solution. Binding proteins which show complete complex formation and form no soluble aggregates are then retested at high concentration (data not shown), in order to predict whether they might be aggregation-prone under crystallization conditions. As last screen, a K_D determination of the binder will help to further rank the selected binders to ensure the isolation of intact complexes. A competition ELISA with several purified DARPins finally reveals whether the binding proteins recognize the same or different, non-overlapping epitopes.

Even without robotic systems, several hundreds of clones can by analyzed by ELISA a day. A SEC-system with an autosampler runs 20–30 samples a day, and with the BioVeris workstation we can determine the binding affinities of around 20 binding proteins a day, both with a minimum of hands-on time. We have developed a workflow that allows us to obtain a characterized binder for co-crystallization within the time period of less than a month.

5. Conclusions

We have selected specific and high-affinity binding molecules to the Na^+-citrate symporter CitS and established an efficient way of characterizing them. All steps of the characterization (ELISA, automated SEC-MALS, affinity determination with BioVeris) are compatible with higher throughput to obtain binding molecules against one or preferentially several membrane proteins. Additionally, the use of two classes of binding molecules is very useful to obtain binders against different epitopes. Therefore, the combination of *in vitro* selection and screening presented here opens up a robust approach for the generation of specific, high-affinity binding molecules suitable for co-crystallization experiments with membrane proteins. Indeed, preliminary results of co-crystallization with selected DARPins seem to corroborate this approach, as well-diffracting crystals of CitS complexes have been obtained.

Acknowledgments

This work was supported by the NCCR Structural Biology. The authors thank Prof. Markus Grütter, Dr. K. Martin Pos, Daniel Frey, Dr. Patrick Amstutz, and Dr. Michael T. Stumpp for helpful discussions.

Appendix A. Supplementary data

Supplementary data associated with this article can be found, in the online version, at doi:10.1016/j.jsb.2007.01.013.

References

Berman, H.M., Westbrook, J., Feng, Z., Gilliland, G., Bhat, T.N., Weissig, H., Shindyalov, I.N., Bourne, P.E., 2000. The Protein Data Bank. Nucleic Acids Res. 28, 235–242.

Binz, H.K., Amstutz, P., Plückthun, A., 2005. Engineering novel binding proteins from nonimmunoglobulin domains. Nat. Biotechnol. 23, 1257–1268.

Binz, H.K., Stumpp, M.T., Forrer, P., Amstutz, P., Plückthun, A., 2003. Designing repeat proteins: well-expressed, soluble and stable proteins from combinatorial libraries of consensus ankyrin repeat proteins. J. Mol. Biol. 332, 489–503.

Binz, H.K., Amstutz, P., Kohl, A., Stumpp, M.T., Briand, C., Forrer, P., Grütter, M.G., Plückthun, A., 2004. High-affinity binders selected from designed ankyrin repeat protein libraries. Nat. Biotechnol. 22, 575–582.

Bork, P., 1993. Hundreds of ankyrin-like repeats in functionally diverse proteins: mobile modules that cross phyla horizontally? Proteins 17, 363–374.

DeLano, W.L., 2002. The PyMOL Molecular Graphics System. DeLano Scientific, Palo Alto, CA, USA. Available from: <<http://www.pymol.org>.

Ewert, S., Huber, T., Honegger, A., Plückthun, A., 2003. Biophysical properties of human antibody variable domains. J. Mol. Biol. 325, 531–553.

Folta-Stogniew, E., Williams, K., 1999. Determination of molecular masses of proteins in solution: Implementation of an HPLC size exclusion chromatography and laser light scattering service in a core laboratory. J. Biomol. Tech. 10, 51–63.

Haenel, C., Satzger, M., Ducata, D.D., Ostendorp, R., Brocks, B., 2005. Characterization of high-affinity antibodies by electrochemiluminescence-based equilibrium titration. Anal. Biochem. 339, 182–184.

Hanes, J., Plückthun, A., 1997. In vitro selection and evolution of functional proteins by using ribosome display. Proc. Natl. Acad. Sci. USA 94, 4937–4942.

Hoogenboom, H.R., 2002. Overview of antibody phage-display technology and its applications. Methods Mol. Biol. 178, 1–37.

Hoogenboom, H.R., 2005. Selecting and screening recombinant antibody libraries. Nat. Biotechnol. 23, 1105–1116.

Hunte, C., Michel, H., 2002. Crystallisation of membrane proteins mediated by antibody fragments. Curr. Opin. Struct. Biol. 12, 503–508.

Kästner, C.N., Dimroth, P., Pos, K.M., 2000. The Na^+-dependent citrate carrier of *Klebsiella pneumoniae*: high-level expression and site-directed mutagenesis of asparagine-185 and glutamate-194. Arch. Microbiol. 174, 67–73.

Kästner, C.N., Prummer, M., Sick, B., Renn, A., Wild, U.P., Dimroth, P., 2003. The citrate carrier CitS probed by single-molecule fluorescence spectroscopy. Biophys. J. 84, 1651–1659.

Kleymann, G., Ostermeier, C., Ludwig, B., Skerra, A., Michel, H., 1995. Engineered Fv fragments as a tool for the one-step purification of integral multisubunit membrane protein complexes. Biotechnology (NY) 13, 155–160.

Knappik, A., Ge, L., Honegger, A., Pack, P., Fischer, M., Wellnhofer, G., Hoess, A., Wölle, J., Plückthun, A., Virnekäs, B., 2000. Fully synthetic human combinatorial antibody libraries (HuCAL) based on modular consensus frameworks and CDRs randomized with trinucleotides. J. Mol. Biol. 296, 57–86.

Lata, S., Piehler, J., 2005. Stable and functional immobilization of histidine-tagged proteins via multivalent chelator headgroups on a molecular poly(ethylene glycol) brush. Anal. Chem. 77, 1096–1105.

Miao, W., Choi, J.P., Bard, A.J., 2002. Electrogenerated chemiluminescence 69: the tris(2,2′-bipyridine)ruthenium(II), $(Ru(bpy)_3^{2+})$/tri-*n*-propylamine (TPrA) system revisited—a new route involving $TPrA^{*+}$ cation radicals. J. Am. Chem. Soc. 124, 14478–14485.

Miroux, B., Walker, J.E., 1996. Over-production of proteins in Escherichia coli: mutant hosts that allow synthesis of some membrane proteins and globular proteins at high levels. J. Mol. Biol. 260, 289–298.

Niebauer, R.T., White, J.F., Fei, Z., Grisshammer, R., 2006. Characterization of monoclonal antibodies directed against the rat neurotensin receptor NTS1. J. Recept. Signal Transduct. Res. 26, 395–415.

Pos, K.M., Dimroth, P., 1996. Functional properties of the purified Na(+)-dependent citrate carrier of *Klebsiella pneumoniae*: evidence for asymmetric orientation of the carrier protein in proteoliposomes. Biochemistry 35, 1018–1026.

Röthlisberger, D., Pos, K.M., Plückthun, A., 2004. An antibody library for stabilizing and crystallizing membrane proteins-selecting binders to the citrate carrier CitS. FEBS Lett. 564, 340–348.

Schwarz, E., Oesterhelt, D., Reinke, H., Beyreuther, K., Dimroth, P., 1988. The sodium ion translocating oxalacetate decarboxylase of *Klebsiella pneumoniae*. Sequence of the biotin-containing alpha-subunit and relationship to other biotin-containing enzymes. J. Biol. Chem. 263, 9640–9645.

Smith, G.P., Petrenko, V.A., 1997. Phage display. Chem. Rev. 97, 391–410.

Sobczak, I., Lolkema, J.S., 2005. The 2-hydroxycarboxylate transporter family: physiology, structure, and mechanism. Microbiol. Mol. Biol. Rev. 69, 665–695.

Steiner, D., Forrer, P., Stumpp, M.T., Plückthun, A., 2006. Signal sequences directing cotranslational translocation expand the range of proteins amenable to phage display. Nat. Biotechnol. 24, 823–831.

Strop, P., Brünger, A.T., 2005. Refractive index-based determination of detergent concentration and its application to the study of membrane proteins. Protein Sci. 14, 2207–2211.

van Geest, M., Lolkema, J.S., 2000. Membrane topology of the Na(+)/citrate transporter CitS of *Klebsiella pneumoniae* by insertion mutagenesis. Biochim. Biophys. Acta 1466, 328–338.

Wallin, E., von Heijne, G., 1998. Genome-wide analysis of integral membrane proteins from eubacterial, archaean, and eukaryotic organisms. Protein Sci. 7, 1029–1038.

Wen, J., Arakawa, T., Philo, J.S., 1996. Size-exclusion chromatography with on-line light-scattering, absorbance, and refractive index detectors for studying proteins and their interactions. Anal. Biochem. 240, 155–166.

Wyatt, P.J., 1993. Light-scattering and the absolute characterization of macromolecules. Anal. Chim. Acta 272, 1–40.